Curr Cardiovasc Imaging Rep (2016) 9: 22
DOI 10.1007/s12410-016-9385-x

CrossMark

CARDIAC NUCLEAR IMAGING (A CUOCOLO, SECTION EDITOR)

Normal Databases for the Relative Quantification of Myocardial Perfusion

Mathieu Rubeaux[1] · **Yuan Xu**[1] · **Guido Germano**[1,2] · **Daniel S. Berman**[1,2] · **Piotr J. Slomka**[1,2]

Published online: 30 June 2016

Abstract
Purpose of Review Myocardial perfusion imaging (MPI) with SPECT is performed clinically worldwide to detect and monitor coronary artery disease (CAD). MPI allows an objective quantification of myocardial perfusion at stress and rest. This established technique relies on normal databases to compare patient scans against reference normal limits. In this review, we aim to introduce the process of MPI quantification with normal databases and describe the associated perfusion quantitative measures that are used.
Recent Findings New equipment and new software reconstruction algorithms have been introduced, which require the development of new normal limits. The appearance and regional count variations of normal MPI scans may differ between these new scanners and standard Anger cameras. Therefore, these new systems may require the determination of new normal limits to achieve optimal accuracy in relative myocardial perfusion quantification. Accurate diagnostic and prognostic results rivaling those obtained by expert readers can be obtained by this widely used technique.
Summary Throughout this review, we emphasize the importance of the normal databases and the need for specific databases relative to distinct imaging procedures. Use of appropriate normal limits allows optimal quantification of MPI by taking into account subtle image differences due to the hardware and software used, and the population studied.

Keywords Single photon emission computed tomography (SPECT) · Myocardial perfusion imaging · Normal databases · Coronary artery disease

Introduction

Objective quantitative analysis is one of the principal strengths of SPECT and PET MPI procedures when compared to other imaging methods. Quantitative analysis has become an established practice in the systematic interpretation of nuclear cardiology studies since early descriptions of the technique for myocardial perfusion imaging (MPI) using SPECT [1, 2]. With the current quantitative approach, analysis of measured values of regional myocardial perfusion for a specific patient requires comparison to corresponding reference values in a normal population. Normal databases for relative distribution of photon count density are thus a necessary component for almost all approaches to quantification of regional hypoperfusion in SPECT MPI studies.

Recently, new SPECT scanners have been introduced [3]. These technologies utilize novel collimations systems and novel software reconstruction techniques incorporating resolution recovery. The appearance and regional count variations of normal MPI scan may differ between these new scanners and standard Anger cameras. Therefore, these new systems require the determination of new normal limits to achieve optimal accuracy in relative myocardial perfusion quantification.

The purpose of this review is to introduce and discuss the concept of normal databases used in MPI quantification in the context of latest hardware developments. We will focus on

This article is part of the Topical Collection on *Cardiac Nuclear Imaging*

✉ Piotr J. Slomka
piotr.slomka@cshs.org

[1] Cedars-Sinai Medical Center, 8700 Beverly Blvd Ste. A047N, Los Angeles, CA 90048, USA

[2] David Geffen School of Medicine, University of California, Los Angeles, CA, USA

SPECT MPI, although most of the issues discussed can apply to PET as well. First, we will review basic concepts of quantification with normal databases. We then present a comparison of the MPI normal databases obtained from several new scanners and new imaging protocols with those previously established for standard SPECT MPI.

Overview of MPI Quantification

Software-based myocardial perfusion quantification has become an integral part of the MPI evaluation. Although the various approaches still require an expert to check image quality and supervise automatic processing, semiquantitative measurements have been shown [4–6] to provide highly reproducible and diagnostically accurate estimates of myocardial perfusion. Routine clinical practice is to combine expert visual analysis and quantitative analysis in case interpretation.

Multiple investigators have developed comprehensive software packages to perform automatic quantification of myocardial perfusion. The examples of clinically validated software programs for quantitative MPI include the Cedars-Sinai QGS + QPS software suite [7], the Emory Cardiac Toolbox [8], the Michigan Corridor 4DM [9], and Wackers-Liu CQ software [10]. The aim of these packages is to automatically provide global and regional measures of myocardial perfusion at stress and rest. The general image processing scheme used in these systems is similar. In particular, most currently used approaches for MPI quantification are based on the local comparisons of the myocardial perfusion samples using polar map coordinates from the patient being tested to the corresponding normal relative perfusion values in the database created from normal scans. This comparison allows the definition of myocardial regions which are hypoperfused and the degree of this hypoperfusion.

The first step in perfusion quantification is the left ventricular myocardium segmentation [7, 11]. Most of the available software tools provide an automatic segmentation of the left ventricle (LV), with manual interaction being necessary in some cases. The LV segmentation is required to isolate the myocardium from surrounding areas of extracardiac activity, such as the liver or bowel. This procedure is typically performed in multiple steps, which include automatic MPI reorientation to standard heart coordinates [12] and automatic detection of myocardial perfusion boundaries. We will not examine thoroughly the algorithms used during the segmentation step as these are well documented [7–10].

Normal Databases and Associated Measures

Figure 1 gives an overview of the quantification process using normal databases as described below.

Polar Sampling and Polar Maps

Once the LV has been segmented, the myocardial uptake is discretized into a limited number of raw perfusion samples represented by the mean or the maximal wall photon counts, for a given point on the myocardial surface [2]. The technical approaches may differ between the different software tools [7–10], but the aim is to express myocardial perfusion in a parametric manner that will facilitate standardized inter-subject comparison. To do so, the sampling scheme usually extracts an equal number of samples in the standard coordinates of the LV for each patient regardless of the true myocardial size and shape.

To facilitate the interpretation of the information extracted by polar sampling, a visual representation called “polar map” or “bull’s eye map” has been developed [13]. This standardized 2D representation of the 3D myocardium allows comparison of studies of different patients on a local, per pixel-basis. Polar maps are extensively used in clinical practice, offering a quick review of myocardial perfusion information for the whole LV in a single image. In addition, polar maps allow a division of the myocardium into regions defined by vascular territories, LV wall, or normalized 17-segment model [14] that are helpful to characterize the defects on a local basis. Although it is possible to quantify myocardial perfusion in 3D on a voxel basis without polar maps [15, 16], most currently used methods utilize the parametric polar-map approach.

Normalization of Counts

Since the quantification of myocardial perfusion is relative in nature, building the polar maps with the raw image counts extracted from the polar sampling requires an additional normalization step to allow an objective comparison between different polar maps (those of the test patient against those in the normal database). Indeed, because scans of different patients may have been obtained with different injected dose and the extracted fraction of the counts by the LV has physiological variation, the level of absolute LV counts can vary greatly. Therefore, the inter-subject normalization method is critical for the overall accuracy of quantification based on the normal limits.

For this purpose, different normalization procedures have been implemented. Simple normalization schemes can produce artifacts and biased variation within the polar maps. For example, the normalization to total counts in the myocardium would over-normalize studies with large defects, while normalization to maximum LV counts or even to a specific percentile of the count range may be skewed by occasional hot spots or heterogeneous distribution of normal counts in the myocardium. Our group has developed a more complex two-pass iterative method allowing normalization to the entire

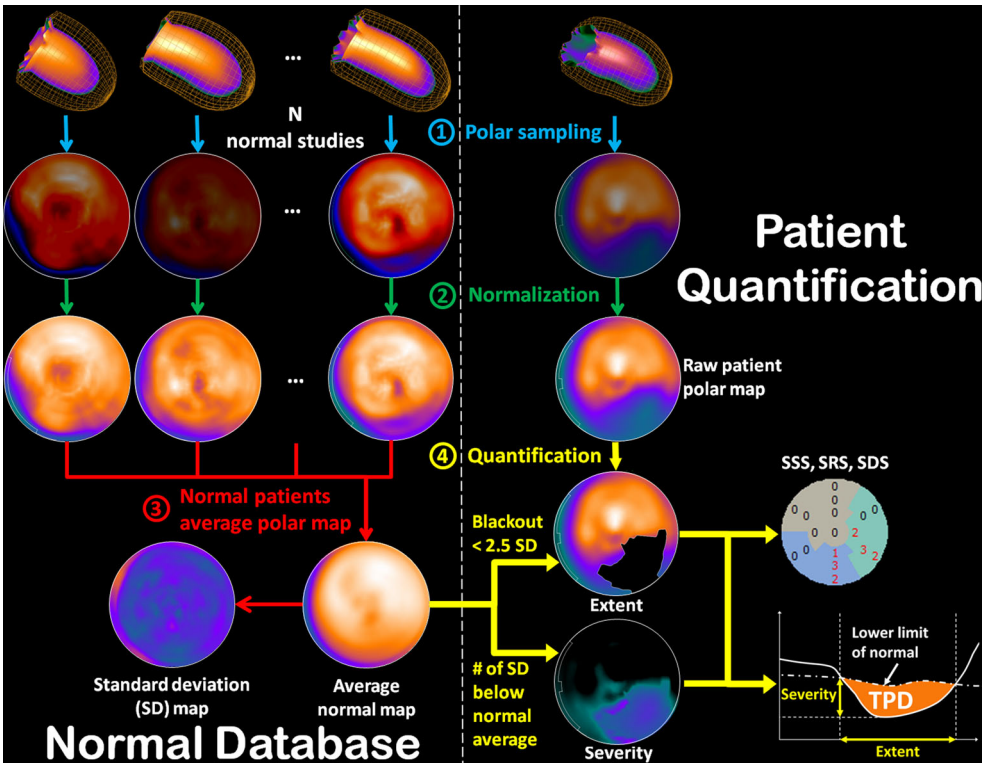

Fig. 1 Illustration of the normal database generation and patient quantification. Polar sampling is used to discretize the patient perfusion information to a finite number of samples represented in a polar map (*step 1*). A normalization step is required to allow a comparison among patients (*step 2*). The normal patients' normalized polar maps are averaged to produce an average and standard deviation normal polar map, constituting the normal database or normal limits (*step 3*). This database is used to compare against the diseased patient, allowing the generation of extent and severity polar maps, which will be used to compute the TPD and the summed scores (*SSS*, *SRS*, and *SDS*) (*step 4*). *TPD* total perfusion deficit, *SSS* summed stress score, *SRS* summed rest score, *SDS* summed difference score

normal region of the myocardium. This method has shown better quantification accuracy than previously utilized percentile techniques [17].

Normal Database Construction

Most quantitative techniques for myocardial perfusion are based on a comparison to normal limits. Practically, a normal database of patients is stored in the form of polar map samples from normal scans. In the Cedars-Sinai software implementation, the raw polar maps of studies used in the databases are stored before normalization and are normalized on-the-fly to a common level during quantification together with the test patient scan. This ensures identical normalizations for both the test patient and the normal database polar maps and allows modifications of the normalization procedure if required. After the normalization step, polar maps of all the patients of the database are averaged to obtain (i) an average normal polar map and (ii) a standard deviation (SD) or absolute deviation map that will serve as the reference to compare against the diseased patient. Absolute deviation representation may be preferred due to non-Gaussian properties of normalized counts.

The normal database is typically comprised of studies from 20 to 40 patients who have a low likelihood of coronary artery disease (<5 to 15 %) and who have had a MPI study which is visually normal. Low likelihood is based on Diamond and Forester criteria [18] which takes into account age, sex, symptoms, and coronary risk factor. The visual assessment of rest and stress studies is performed and patients with abnormal scans despite the low likelihood of disease are excluded.

Usually, the normal database is specific to a type of camera, detector, acquisition protocol, and even patient gender, since the normal distribution of males and females can be significantly different [19]. Moreover, since the perfusion quantification relies on a comparison between stress and rest images, specific rest and stress normal databases are commonly employed. Furthermore, since the radiopharmaceutical used during the exam will also influence the normal databases, tracer-specific databases are also generated. Several databases are usually provided together with the quantitative software which comprises some tools that allow the generation of the normal databases by the users if required.

Quantification

The resulting average normalized polar maps of the normal patients are subsequently statistically compared to the polar map of the test patient on a pixel-by-pixel basis, and the differences are shown as color-coded parametric images. Typically, at least two new polar maps are created after the comparison to normal limits, namely the extent (or blackout) and severity maps [20]. The extent map represents the proportion of the myocardial volume with hypoperfusion, while the severity map represents the degree of the hypoperfusion. The combination of the extent and severity of perfusion

abnormalities has been shown to provide the greatest prognostic value of MPI.

The blackout polar map is created by setting the pixel of the patient polar map to 0 (black color) when its normalized counts are lower than a certain threshold below the normal database mean polar map. Typically, a threshold based on difference from the mean—for example 2.5 SD below (or approximately equivalent 3 mean absolute deviations)—of the normal distribution of counts in this pixel is used. The blackout map allows the reader to quickly see the location and size of the hypoperfusion defect [21]. Since the polar map can be divided into areas such as vascular regions or the 17-segment model [14], the degree of hypoperfusion can be expressed locally as a percentage of the total defect belonging to a given region or segment. The severity polar map is expressed as the number of standard deviations or mean absolute deviations below the normal mean [21] and gives a local measure of the depth (severity) of the hypoperfusion. It can also be computed in a regional or global fashion.

Using these parametric polar maps, a measure estimating the overall magnitude of myocardial hypoperfusion—total perfusion deficit (TPD)—has been developed [17]. TPD is a computer-derived analogue of the visual percent myocardium that is abnormal by visual analysis and combines both defect extent and severity. An illustration of the TPD computation is given at the bottom right of Fig. 1. It shows a circumferential profile for one short axis slice with the corresponding normal limit obtained from the normal database. The area below the normal limit curve and above the circumferential profile curve defines the perfusion deficit for that slice. Summing all the perfusion deficits from all circumferential profiles gives TPD. TPD is measured at stress and rest, and ischemic TPD can be defined by the difference between stress and rest TPD. The reproducibility of stress, rest, and ischemic TPD obtained by automatic quantification has been demonstrated to be superior to visual percent myocardium assessment [17].

Well-validated visual measures of segmental and global hypoperfusion are routinely used by physicians clinically to determine magnitude of hypoperfusion. These are summed stress score (SSS), summed rest score (SRS), and summed difference score (SDS) [22]. Like TPD, these measures also combine the severity and extent of perfusion defects during stress and rest [23]. SSS is a semiquantitative score obtained by adding the individual scores derived from the 17 segments that are analyzed and scored during a stress study. Each of the 17 segments is scored on a 5-point scale: 0 = normal, 1 = equivocal, 2 = significant abnormality, 3 = severe reduction of uptake, and 4 = absence of uptake [14]. In standard clinical practice, SSS <4 indicates a lack of significant abnormality, while higher SSS reflects greater extent and severity of perfusion defects, a SSS >13 representing a severe abnormality. The SRS is obtained analogously from the rest study. The SDS, expressed as the difference between SSS and SRS, indicates the amount of reversibly hypoperfused myocardium (generally referred to as the ischemic myocardium) and the degree of reversibility. As an aid to clinicians, these scores can also be obtained automatically [17] from the severity maps, by computing appropriately calibrated average pixel abnormality scores within each segment of the 17-segment model. In general, the TPD measure is highly correlated with the SSS or SRS scores, but some differences can occur due to discretization of counts into segments and due to the rounding to integer scores [17]. Usually, a study is deemed to be abnormal if comparison to the normal distribution demonstrates that the patient's stress perfusion distribution exhibits more than 3 to 5 % TPD (depending on the imaging protocol) or a summed stress score ≥4 [24].

Direct Change Quantification

Normal databases represent the strength as well as the weakness of the quantitative approach. They have been shown to be very effective and reproducible, giving similar diagnostic prediction as a trained observer. However, as noted above, a new database is usually required for new types of scanner or new imaging protocols. Therefore, most of the available software solutions allow the user to create site-specific normal databases. To avoid the use of normal databases, alternative measures have been developed using stress and rest or serial stress scans of the patient to obtain some measure of change in hypoperfusion. A global measure reflecting the stress-rest change and allowing a direct estimation of ischemia from stress and rest images was proposed and shown to be diagnostically useful [25]. It is calculated as the ratio of the total deficit LV counts to the total rest LV counts, after an iterative registration procedure of the stress and rest images and taking into account the count normalization of both images. This approach can be used as a complementary technique to the standard method using normal databases.

New Developments and the Need for Specific Databases

Recent MPI SPECT developments are aimed at reducing the attenuation artifacts [26], as well as reducing imaging time and radiation exposure for the patient [27]. New scanners with solid-state detectors and specialized collimators have been introduced with improved sensitivity and image resolution. Low-dose protocols are becoming used in routine clinical practice. To reduce attenuation artifacts, CT attenuation correction [28] or 2-position imaging [29–31] (where the patient is imaged in prone/supine or upright/supine positions) have been introduced. These improvements have increased the complexity of myocardial perfusion quantification, requiring additional normal limits (limits with and without attenuation

correction as well as specific limits for a particular imaging position).

New Scanner Databases

Recently introduced high efficiency cameras with specialized collimators and solid-state cadmium-zinc-telluride (CZT) detectors have demonstrated a good potential in MPI, improving image quality, shortening imaging time, while considerably lowering the radiation dose [3, 32, 33]. The reader can refer to [3, 34] for an overview of the new hardware and reconstruction approaches. The CZT cameras have been validated clinically and show similar overall diagnostic accuracy to standard cameras when compared to coronary angiography [34, 35]. For quantitative analysis, normal databases for new scanners have been generated by several groups, for example for the Discovery NM 530c (GE Healthcare) [36–38] and D-SPECT (Spectrum-Dynamics) [31, 39•, 40••] cameras.

While these studies demonstrated equal or even superior quantitative analysis using the CZT systems as compared to conventional cameras [31, 36, 37, 39•], only one study to date to our knowledge has examined in detail the characteristics of the normal limits generated for these new systems [40••]. This multicenter trial compared conventional and CZT databases created for a D-SPECT camera, which utilizes semi-upright as well as supine imaging. With upright imaging using D-SPECT camera, as compared to standard Anger camera supine images, higher count rates were observed in the anterior and mid-inferior inferoseptal segments in men, and higher count rates were seen in the anterior wall but lower counts in the inferior segments in women. The authors concluded that these differences can be partially attributed to the sitting acquisition position that influences the position of the attenuating tissues (diaphragm and abdominal fat tissue for the men, breast tissue for the women) relative to the heart. This finding should be taken into account when imaging with semi-upright as well as upright imaging approaches.

Low-Dose Databases

With these new imaging systems, very low-dose imaging is now possible. Several groups [32, 41••, 42, 43] showed the applicability of low doses (ranging from 1 to 6 mSv) for quantitative analysis. But, the use of low dose normal databases is not yet standardized. In some studies, low-dose normal limits are used [41••, 43], while Sharir et al. [42] uses combined low-dose and normal dose patients to build the normal database. List-mode acquisition allows for a unique manner of exploring the effects of lowering counts on quantitative MPI analysis. Nakazato et al. developed simulated count-specific normal limits by reframing the normal patients' list-mode raw data [41••]. In comparison with using the same normal limits for different count levels, these count-specific normal limits allow a significant reduction of TPD bias when lowering the dose, as shown in Fig. 2. Thus, count-specific normal limits will allow to obtain comparable quantitative findings for studies with different count levels, since the normal thresholds for perfusion studies can be affected by the bias. As far as we know, this is the only study that specifically evaluated the effect of the reducing counts on the quantitative analysis. This methodology lends itself to further studies on low-dose MPI.

Attenuation Correction

Attenuation correction (AC) has been developed to reduce photon attenuation and associated artifacts, and most camera manufacturers now provide hardware and software implementations of AC protocols, which have been tested in several validation studies [5, 44–46]. Usually, an attenuation map of density differences throughout the body is constructed from a CT scan of the patient, and this map is then used to correct for the absorption of the photons in the SPECT image. AC SPECT images will differ from non-corrected images and therefore require specific normal databases. A number of AC specific databases have been characterized [19, 46–49]. Several studies show diagnostic improvement in the use of AC compared to non-corrected images, and AC imaging has been recommended for clinical practice [50]. It has been suggested that the gender-specific normal limits may not be required for AC studies if the main differences between male and female databases could be attributed to the different patterns of photon attenuation [47, 48]. However, while some of the studies show no significant differences between male and female AC normal databases [47, 48], others do [19, 49]. This divergence may be due to the number of patients integrated in the databases, as well as other protocol-dependent factors. Further investigations are needed to elucidate whether gender-specific databases are needed for AC images.

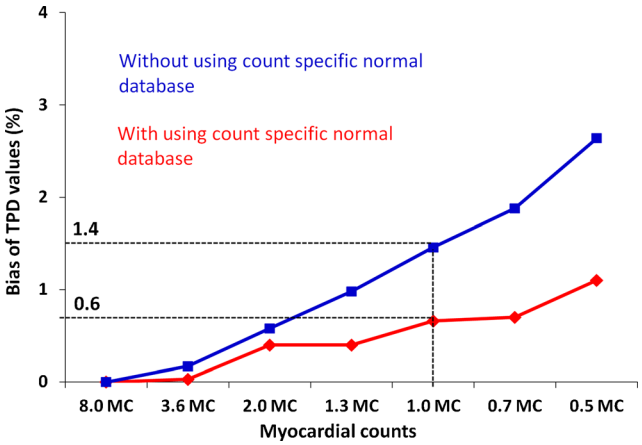

Fig. 2 Total perfusion deficit (*TPD*) bias as a function of decreasing count levels with (*red*) and without (*blue*) count-specific normal limits. This research was originally published in Nakazato et al. [41••] © by the Society of Nuclear Medicine and Molecular Imaging, Inc.

Table 1 MPI protocols, scanners, and patient information for the presented normal databases

	Number of patients	Age	BMI	Rest dose (mCi)	Stress dose (mCi)
Conventional (NC/AC)					
Female	49	57 ± 18	30 ± 11	8 − 12	29 − 42
Male	50	55 ± 11	31 ± 6	8 − 12	29 − 42
Astonish (NC/AC)					
Female	40	53 ± 8	30 ± 6	10	25 − 35
Male	40	54 ± 9	28 ± 6	10	25 − 35
Cardius XPO (NC/AC)					
Female	50	53 ± 11	31 ± 10	8 − 12	24 − 36
Male	38	53 ± 10	30 ± 7	8 − 12	24 − 36
D-SPECT (NC)					
Female	30	53 ± 11	29 ± 7	8 − 9	36 − 40
Male	30	59 ± 14	27 ± 7	8 − 9	36 − 40
Discovery NM 530c (NC)					
Female	29	61 ± 13	26 ± 5	5 − 8	15 − 24
Male	34	56 ± 11	29 ± 7	5 − 8	15 − 24

All patients followed sestamibi Tc-99m rest/stress protocols. Conventional indicates Vertex standard Anger camera, standard iterative reconstruction (Philips Medical Systems). Astonish indicates Cardio MD standard Anger camera with Astonish resolution recovery reconstruction protocol (Philips Medical Systems). Cardius XPO indicates solid-state camera (Digirad). D-SPECT indicates CZT camera (Spectrum-Dynamics). Discovery NM 530c indicates CZT camera (GE Healthcare).

AC attenuation correction, *NC* without attenuation correction

Dual Position Imaging

Another way to compensate for photon attenuation was introduced with 2-position imaging [29, 51, 52]. By comparing MPI images taken with patient in two different positions, it becomes easier to isolate attenuation artifacts from true perfusion defects. This approach can be also utilized in combined 2-position MPI quantification [53, 54] and is recommended when AC is not available, which is common on newer dedicated cardiac SPECT CZT scanners [31]. Normal databases for these new protocols have been successfully developed by multiple teams [31, 38, 39•]. While separate supine and prone normal limits have been developed, a study by Nakazato et al. [31] suggests that the reference limits for upright and supine data with CZT cameras can be combined, likely because of the lower variability between upright and supine positions, as compared to prone/supine positions. Thus, the same normal limits could be used for upright/supine imaging, but this may need to be confirmed by further studies.

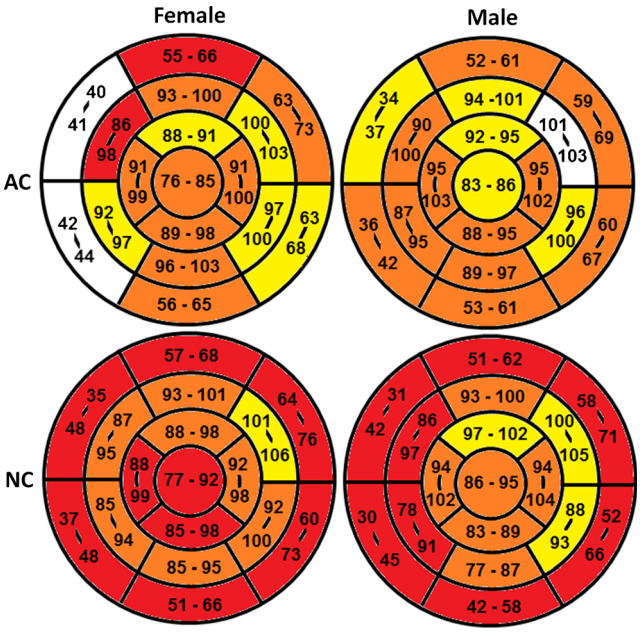

Fig. 3 Color-coded average range of normalized uptake across all stress databases from Table 1. Databases were created with QPS software. ≤2 % (*white*), 2 % < range ≤ 5 % (*yellow*), 5 % < range ≤ 10 % (*orange*), and >10 % (*red*). *AC* attenuation correction, *NC* without attenuation correction

Population-Specific Database

Apart from the protocol or technologies that will influence the need for specific normal databases, the patients' characteristics must also be taken into account. Since most of the development of MPI software packages has taken place in the USA, the databases integrated into these solutions for the most part reflect western population. However, possible differences mostly due to body habitus should be taken into account. For example, the Japanese Society of Nuclear Medicine has recently performed an extensive validation of Japanese-specific databases [55–57, 58•], clearly demonstrating the

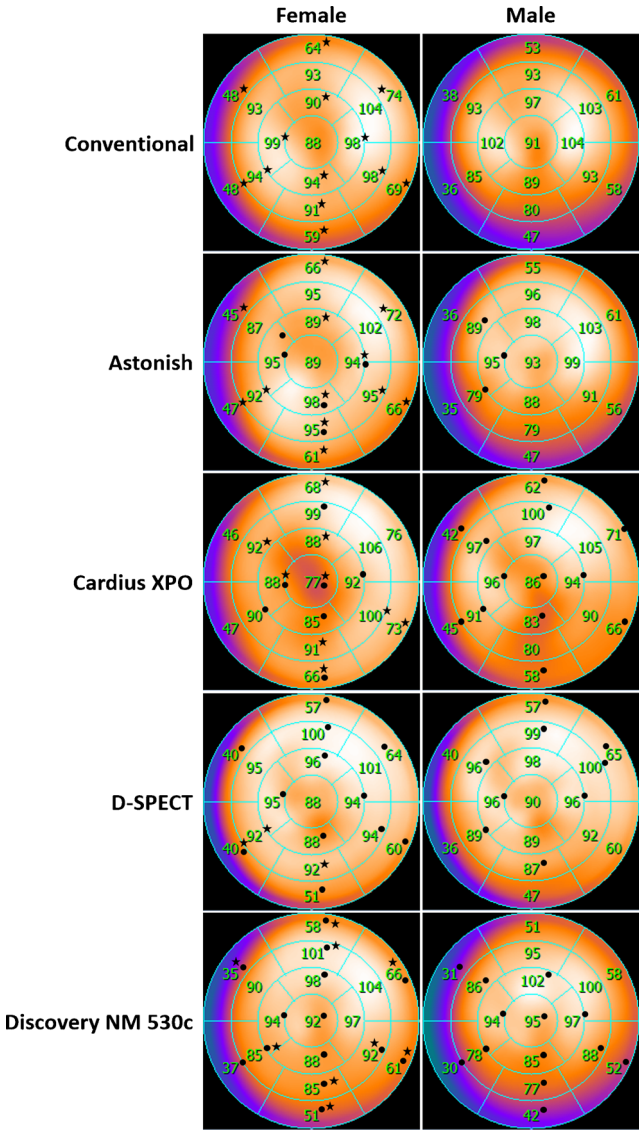

Fig. 4 Comparison of stress databases without attenuation correction (NC) from Table 1, showing significant statistical differences. All databases vs conventional (*circle*) and female vs male (*star*). Conventional indicates Vertex standard Anger camera (Philips Medical Systems). Astonish indicates Cardio MD standard Anger camera with Astonish resolution recovery reconstruction protocol (Philips Medical Systems). Cardius XPO indicates solid-state camera (Digirad). D-SPECT indicates CZT camera (Spectrum-Dynamics). Discovery NM 530c indicates CZT camera (GE Healthcare)

need for building region-specific databases. Other examples include Chinese- [59] or Spanish- [60] specific databases. Nevertheless, a study of a French population [37] showed no particular difference between the population-specific and the vendor-supplied normal databases. An explanation could be that the body habitus of French patients are not that different from North America ones.

Other patient specificities can be also taken into account when building normal limits. In a recent study [61••], a normal database has been built and proved to be efficient for patients with end-stage renal disease. Most likely, the need for a different database in these patients relates to the common presence of severe left ventricular hypertrophy associated with renal failure and its consequent hypertension. Increased count intensity in the septal wall on myocardial perfusion is observed, likely due to a partial volume effect of secondary to left ventricular hypertrophy. This finding is also likely to apply to other populations with left ventricular hypertrophy. Similar work could be extended to other pathologies with specific myocardial perfusion signatures, leading to disease-specific databases.

Finally, obese patients are of particular interest when dealing with MPI, because they are more likely to face cardiovascular diseases and cardiac mortality [62]. Imaging of obese patients may lead to higher incidence of attenuation artifacts and produce artificial myocardial perfusion defects compared to non-obese patients [63, 64]. Studies have been conducted recently to determine the applicability of new CZT cameras [39•, 65, 66] to obese patients. While specific normal databases generated for obese patients have been tested with conventional cameras, showing no significant differences [19] as compared to non-obese patients normal databases, this investigation has not yet been conducted on the new CZT cameras.

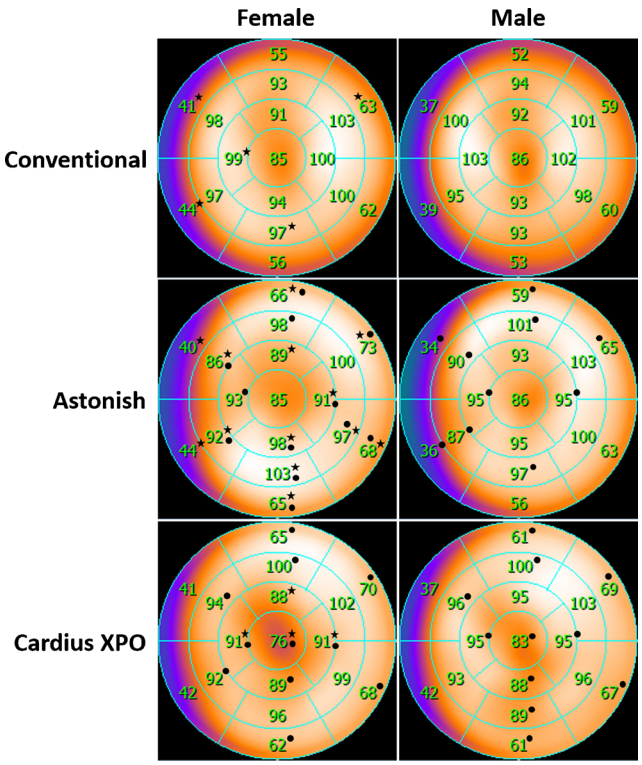

Fig. 5 Comparison of stress databases with attenuation correction (AC) from Table 1, showing significant statistical differences. All databases vs conventional (*circle*) and female vs male (*star*). Conventional indicates Vertex standard Anger camera (Philips Medical Systems). Astonish indicates Cardio MD standard Anger camera with Astonish resolution recovery reconstruction protocol (Philips Medical Systems). Cardius XPO indicates solid-state camera (Digirad)

Variability of Normal Databases

To illustrate the possible differences between various system-, gender- and protocol-specific databases, we show a comparison of several normal databases, created from scans acquired by different methods described above (Table 1). The databases have been created with the QPS Cedars-Sinai software.

These studies were performed using sestamibi technetium 99m (Tc-99m) rest and sestamibi Tc-99m stress protocols, but only stress databases are presented here. In addition, to focus on imaging protocols and scanners differences, databases are shown just for one tracer (sestamibi Tc-99m). The limits were created separately for males and females for all systems. Databases with AC are also shown, except for the CZT systems (D-SPECT and Discovery NM 530c) for which this option was not available. The criterion of inclusion to the database was a low likelihood of coronary artery disease based on traditional risk assessment and visually normal perfusion scan. The number of patients for each database ranged between 29 and 50.

The mean normalized regional myocardial uptakes were derived for each database and each gender, and displayed with a standard 17-segment model for all databases [14]. Figure 3 gives the ranges of mean normalized uptakes for all databases for each gender with/without AC. This clearly shows that AC helps reducing the variability across databases. The polar map depictions of low-likelihood male and female stress databases without AC are shown in Fig. 4. We found significant differences ($p < 0.05$) in the basal and apex regions between females and males in the standard database. In the databases generated from the new technology scanners, the differences in each segment between genders decreased most notably for D-SPECT and Cardius XPO systems. There were significant differences in most segments between the new scanner databases and the standard camera database. The polar map depictions of low-likelihood male and female stress databases with AC are shown in Fig. 5. Compared to non-corrected standard databases, only a few significant differences in the basal and apex regions between females and males in the conventional AC database could be found. In the database with resolution recovery (Astonish), there were significant differences in most areas (especially basal and apex regions) between females and males. In the database for Cardius XPO, the only significant differences between females and males were at the apex region. Similar to comparison in non-corrected databases, there were also significant differences in most segments between the AC databases for advanced technologies and standard AC databases.

Conclusions

Relative quantification of myocardial perfusion is a mainstay of the nuclear cardiology. Accurate diagnostic and prognostic results rivaling those obtained by expert readers can be obtained by this widely used technique. The use of appropriate normal limits allows optimal quantification of MPI by taking into account subtle image differences due to the hardware and software used, and the population studied. Such precise calibration of the perfusion findings is not easy for the visual observer. Normal databases may differ for the chosen patient population, hardware, isotope, and protocol and can be generated by the users if required. However, generic databases are likely to be useful for specific common protocols and scanner configurations. The importance of the normal limits has to be kept in mind because the accuracy of the final quantitative results may depend on the selection of the normal databases.

Compliance with Ethical standards

Conflict of Interest MR and YX declare that they have no conflicts of interest. Cedars-Sinai Medical Center receives royalties for the quantitative assessment of function, perfusion, and viability, a minority portion of which is distributed to some of the authors of this manuscript (GG, DSB, and PJS). PJS also reports grants from Siemens, outside the submitted work.

Human and Animal Rights and Informed Consent All reported studies/experiments with human or animal subjects performed by the authors have been previously published and complied with all applicable ethical standards (including the Helsinki declaration and its amendments, institutional/national research committee standards, and international/national/institutional guidelines).

Funding This research was supported in part by grant R01HL089765 from the National Heart, Lung, and Blood Institute/National Institutes of Health (NHLBI/NIH) (PI: PJS). Also, YX is now affiliated with the School of Nursing, University of California, San Francisco, CA.

References

Papers of particular interest, published recently, have been highlighted as:
- • Of importance
- •• Of major importance

1. Garcia E, Maddahi J, Berman D, Waxman A. Space/time quantitation of thallium-201 myocardial scintigraphy. J Nucl Med. 1981;22(4):309–17.
2. Garcia EV, Van Train K, Maddahi J, Prigent F, Friedman J, Areeda J, et al. Quantification of rotational thallium-201 myocardial tomography. J Nucl Med. 1985;26(1):17–26.
3. Slomka PJ, Patton JA, Berman DS, Germano G. Advances in technical aspects of myocardial perfusion SPECT imaging. J Nucl Cardiol. 2009;16(2):255–76. doi:10.1007/s12350-009-9052-6.

4. Berman DS, Kang X, Gransar H, Gerlach J, Friedman JD, Hayes SW, et al. Quantitative assessment of myocardial perfusion abnormality on SPECT myocardial perfusion imaging is more reproducible than expert visual analysis. J Nucl Cardiol. 2009;16(1):45–53. doi:10.1007/s12350-008-9018-0.
5. Arsanjani R, Xu Y, Hayes SW, Fish M, Lemley Jr M, Gerlach J, et al. Comparison of fully automated computer analysis and visual scoring for detection of coronary artery disease from myocardial perfusion SPECT in a large population. J Nucl Med. 2013;54(2):221–8. doi:10.2967/jnumed.112.108969.
6. Wolak A, Slomka PJ, Fish MB, Lorenzo S, Acampa W, Berman DS, et al. Quantitative myocardial-perfusion SPECT: comparison of three state-of-the-art software packages. J Nucl Cardiol. 2008;15(1):27–34.
7. Germano G, Kavanagh PB, Slomka PJ, Van Kriekinge SD, Pollard G, Berman DS. Quantitation in gated perfusion SPECT imaging: the Cedars-Sinai approach. J Nucl Cardiol. 2007;14(4):433–54.
8. Garcia EV, Faber TL, Cooke CD, Folks RD, Chen J, Santana C. The increasing role of quantification in clinical nuclear cardiology: the Emory approach. J Nucl Cardiol. 2007;14(4):420–32.
9. Ficaro EP, Lee BC, Kritzman JN, Corbett JR. Corridor4DM: the Michigan method for quantitative nuclear cardiology. J Nucl Cardiol. 2007;14(4):455–65.
10. Liu YH. Quantification of nuclear cardiac images: the Yale approach. J Nucl Cardiol. 2007;14(4):483–91.
11. Faber TL, Cooke CD, Folks RD, Vansant JP, Nichols KJ, DePuey EG, et al. Left ventricular function and perfusion from gated SPECT perfusion images: an integrated method. J Nucl Med. 1999;40(4):650–9.
12. Germano G, Kavanagh PB, Su HT, Mazzanti M, Kiat H, Hachamovitch R, et al. Automatic reorientation of three-dimensional, transaxial myocardial perfusion SPECT images. J Nucl Med. 1995;36(6):1107–14.
13. Caldwell JH, Williams DL, Harp GD, Stratton JR, Ritchie JL. Quantitation of size of relative myocardial perfusion defect by single-photon emission computed tomography. Circulation. 1984;70(6):1048–56.
14. Cerqueira MD, Weissman NJ, Dilsizian V, Jacobs AK, Kaul S, Laskey WK, et al. Standardized myocardial segmentation and nomenclature for tomographic imaging of the heart: a statement for healthcare professionals from the Cardiac Imaging Committee of the Council on Clinical Cardiology of the American Heart Association. Circulation. 2002;105(4):539–42.
15. Slomka PJ, Hurwitz GA, Stephenson J, Cradduck T. Automated alignment and sizing of myocardial stress and rest scans to three-dimensional normal templates using an image registration algorithm. J Nucl Med. 1995;36(6):1115–22.
16. Declerck J, Feldmar J, Goris ML, Betting F. Automatic registration and alignment on a template of cardiac stress and rest reoriented SPECT images. IEEE Trans Med Imaging. 1997;16(6):727–37.
17. Slomka PJ, Nishina H, Berman DS, Akincioglu C, Abidov A, Friedman JD, et al. Automated quantification of myocardial perfusion SPECT using simplified normal limits. J Nucl Cardiol. 2005;12(1):66–77.
18. Diamond GA, Forrester JS. Analysis of probability as an aid in the clinical diagnosis of coronary-artery disease. N Engl J Med. 1979;300:1350–8.
19. Slomka PJ, Fish MB, Lorenzo S, Nishina H, Gerlach J, Berman DS, et al. Simplified normal limits and automated quantitative assessment for attenuation-corrected myocardial perfusion SPECT. J Nucl Cardiol. 2006;13(5):642–51.
20. Van Train KF, Areeda J, Garcia EV, Cooke CD, Maddahi J, Kiat H, et al. Quantitative same-day rest-stress technetium-99m-sestamibi SPECT: definition and validation of stress normal limits and criteria for abnormality. J Nucl Med. 1993;34(9):1494–502.
21. Slomka P, Xu Y, Berman D, Germano G. Quantitative analysis of perfusion studies: strengths and pitfalls. J Nucl Cardiol. 2012;19(2):338–46. doi:10.1007/s12350-011-9509-2.
22. Berman DS, Hachamovitch R, Kiat H, Cohen I, Cabico JA, Wang FP, et al. Incremental value of prognostic testing in patients with known or suspected ischemic heart disease: a basis for optimal utilization of exercise technetium-99m sestamibi myocardial perfusion single-photon emission computed tomography. J Am Coll Cardiol. 1995;26(3):639–47.
23. Berman DS, Kiat H, Friedman JD, Wang FP, van Train K, Matzer L, et al. Separate acquisition rest thallium-201/stress technetium-99m sestamibi dual-isotope myocardial perfusion single-photon emission computed tomography: a clinical validation study. J Am Coll Cardiol. 1993;22(5):1455–64.
24. Berman D, Abidov A, Kang X, Hayes SW, Friedman J, Sciammarella M et al. Prognostic Validation of a 17-Segment Score Derived from a 20-Segment Score for Myocardial Perfusion SPECT Interpretation. J Nucl Cardiol. 2004 (accepted).
25. Slomka PJ, Nishina H, Berman DS, Kang X, Friedman JD, Hayes SW, et al. Automatic quantification of myocardial perfusion stress-rest change: a new measure of ischemia. J Nucl Med. 2004;45(2):183–91.
26. Heller GV, Bateman TM, Johnson LL, Cullom SJ, Case JA, Galt JR, et al. Clinical value of attenuation correction in stress-only Tc-99m sestamibi SPECT imaging. J Nucl Cardiol. 2004;11(3):273–81. doi:10.1016/j.nuclcard.2004.03.005.
27. Bateman TM, Heller GV, McGhie AI, Courter SA, Golub RA, Case JA, et al. Multicenter investigation comparing a highly efficient half-time stress-only attenuation correction approach against standard rest-stress Tc-99m SPECT imaging. J Nucl Cardiol. 2009;16(5):726–35.
28. Herzog BA, Buechel RR, Husmann L, Pazhenkottil AP, Burger IA, Wolfrum M, et al. Validation of CT attenuation correction for high-speed myocardial perfusion imaging using a novel cadmium-zinc-telluride detector technique. J Nucl Med. 2010;51(10):1539–44. doi:10.2967/jnumed.110.078170.
29. Berman DS, Kang X, Nishina H, Slomka PJ, Shaw LJ, Hayes SW, et al. Diagnostic accuracy of gated Tc-99m sestamibi stress myocardial perfusion SPECT with combined supine and prone acquisitions to detect coronary artery disease in obese and nonobese patients. J Nucl Cardiol. 2006;13(2):191–201.
30. Hayes SW, De Lorenzo A, Hachamovitch R, Dhar SC, Hsu P, Cohen I, et al. Prognostic implications of combined prone and supine acquisitions in patients with equivocal or abnormal supine myocardial perfusion SPECT. J Nucl Med. 2003;44(10):1633–40.
31. Nakazato R, Tamarappoo BK, Kang X, Wolak A, Kite F, Hayes SW, et al. Quantitative upright-supine high-speed SPECT myocardial perfusion imaging for detection of coronary artery disease: correlation with invasive coronary angiography. J Nucl Med. 2010;51(11):1724–31.
32. Einstein AJ, Blankstein R, Andrews H, Fish M, Padgett R, Hayes SW, et al. Comparison of image quality, myocardial perfusion, and left ventricular function between standard imaging and single-injection ultra-low-dose imaging using a high-efficiency SPECT camera: the MILLISIEVERT Study. J Nucl Med. 2014;55(9):1430–7. doi:10.2967/jnumed.114.138222.
33. Mouden M, Timmer JR, Ottervanger JP, Reiffers S, Oostdijk AH, Knollema S, et al. Impact of a new ultrafast CZT SPECT camera for myocardial perfusion imaging: fewer equivocal results and lower radiation dose. Eur J Nucl Med Mol Imaging. 2012;39(6):1048–55. doi:10.1007/s00259-012-2086-z.
34. Garcia EV, Faber TL, Esteves FP. Cardiac dedicated ultrafast SPECT cameras: new designs and clinical implications. J Nucl Med. 2011;52(2):210–7. doi:10.2967/jnumed.110.081323.
35. Sweeny JM, Baber U, Croft LB, High-efficiency GKA, SPECT MPI. Comparison of automated quantification, visual interpretation, and coronary angiography. J Nucl Cardiol. 2013;20:763–73.

36. Duvall WL, Slomka PJ, Gerlach JR, Sweeny JM, Baber U, Croft LB, et al. High-efficiency SPECT MPI: comparison of automated quantification, visual interpretation, and coronary angiography. J Nucl Cardiol. 2013;20(5):763–73. doi:10.1007/s12350-013-9735-x.
37. Gregoire B, Pina-Jomir G, Bontemps L, Janier M, Scheiber C. The value of local normal limits in quantitative Thallium-201 CZT MPI SPECT. J Nucl Cardiol. 2016. doi:10.1007/s12350-016-0430-6.
38. Nishiyama Y, Miyagawa M, Kawaguchi N, Nakamura M, Kido T, Kurata A, et al. Combined Supine and Prone Myocardial Perfusion Single-Photon Emission Computed Tomography With a Cadmium Zinc Telluride Camera for Detection of Coronary Artery Disease. Circ J. 2014;78(5):1169–75. doi:10.1253/circj.CJ-13-1316.
39.• Nakazato R, Slomka PJ, Fish M, Schwartz RG, Hayes SW, Thomson LE, et al. Quantitative high-efficiency cadmium-zinc-telluride SPECT with dedicated parallel-hole collimation system in obese patients: results of a multi-center study. J Nucl Cardiol. 2014. doi:10.1007/s12350-014-9984-3. **This study presents the construction of a normal database for obese patients using new CZT cameras. It showed that new CZT cameras allow high image quality and accurate quantitative analysis of obese patients**.
40.•• Sharir T, Slomka PJ, Hayes SW, DiCarli MF, Ziffer JA, Martin WH, et al. Multicenter trial of high-speed versus conventional single-photon emission computed tomography imaging: quantitative results of myocardial perfusion and left ventricular function. J Am Coll Cardiol. 2010;55(18):1965–74. **This is the first multicenter trial comparing characteristics of the normal databases constructed from CZT (D-SPECT) and conventional Anger cameras. It shows differences in the count rates of the 17 segment model that can be partially explained by the specific (sitting) position of the D-SPECT system**.
41.•• Nakazato R, Berman D, Hayes M, Fish M, Padgett R, Xu Y, et al. Myocardial perfusion imaging with a solid state camera: simulation of a very low dose imaging protocol. J Nucl Med. 2013;54(3):373–9. **This is the first study simulating count-specific normal databases in the context of very low dose imaging. These specific normal limits allow a significant reduction of the TPD bias**.
42. Sharir T, Pinskiy M, Pardes A, Rochman A, Prokhorov V, Kovalski G, et al. Comparison of the diagnostic accuracies of very low stress-dose with standard-dose myocardial perfusion imaging: automated quantification of one-day, stress-first SPECT using a CZT camera. J Nucl Cardiol. 2015;23(1):11–20. doi:10.1007/s12350-015-0130-7.
43. Esteves FP, Galt JR, Folks RD, Verdes L, Garcia EV. Diagnostic performance of low-dose rest/stress Tc-99m tetrofosmin myocardial perfusion SPECT using the 530c CZT camera: quantitative vs visual analysis. J Nucl Cardiol. 2014;21(1):158–65. doi:10.1007/s12350-013-9827-7.
44. Links JM, DePuey EG, Taillefer R, Becker LC. Attenuation correction and gating synergistically improve the diagnostic accuracy of myocardial perfusion SPECT. J Nucl Cardiol. 2002;9(2):183–7.
45. Thompson RC, Heller GV, Johnson LL, Case JA, Cullom SJ, Garcia EV, et al. Value of attenuation correction on ECG-gated SPECT myocardial perfusion imaging related to body mass index. J Nucl Cardiol. 2005;12(2):195–202.
46. Xu YA, Fish M, Gerlach J, Lemley M, Berman DS, Germano G, et al. Combined quantitative analysis of attenuation corrected and non-corrected myocadial perfusion SPECT: method development and clinical validation. J Nucl Cardiol. 2010;17(4):591–9. doi:10.1007/s12350-010-9220-8.
47. Grossman GB, Garcia EV, Bateman TM, Heller GV, Johnson LL, Folks RD, et al. Quantitative Tc-99m sestamibi attenuation-corrected SPECT: development and multicenter trial validation of myocardial perfusion stress gender-independent normal database in an obese population. J Nucl Cardiol. 2004;11(3):263–72.
48. Ficaro EP, Fessler JA, Shreve PD, Kritzman JN, Rose PA, Corbett JR. Simultaneous transmission/emission myocardial perfusion tomography: diagnostic accuracy of Attenuation-Corrected 99mTc-SestamibiSingle-Photon Emission Computed Tomography. Circulation. 1996;93(3):463–73.
49. Tragardh E, Sjostrand K, Jakobsson D, Edenbrandt L. Small average differences in attenuation corrected images between men and women in myocardial perfusion scintigraphy: a novel normal stress database. BMC Med Imaging. 2011;11:18. doi:10.1186/1471-2342-11-18.
50. Heller GV, Links J, Bateman TM, Ziffer JA, Ficaro E, Cohen MC, et al. American Society of Nuclear Cardiology and Society of Nuclear Medicine joint position statement: attenuation correction of myocardial perfusion SPECT scintigraphy. J Nucl Cardiol. 2004;11(2):229–30.
51. Kiat H, Van Train KF, Friedman JD, Germano G, Silagan G, Wang FP, et al. Quantitative stress-redistribution thallium-201 SPECT using prone imaging: methodologic development and validation. J Nucl Med. 1992;33(8):1509–15.
52. Hayes SW, De Lorenzo A, Hachamovitch R, Dhar SC, Hsu P, Cohen I, et al. Prognostic implications of combined prone and supine acquisitions in patients with equivocal or abnormal supine myocardial perfusion SPECT. J Nucl Med. 2003;44(10):1633–40.
53. Nishina H, Slomka PJ, Abidov A, Yoda S, Akincioglu C, Kang X et al. Combined supine and prone quantitative myocardial perfusion SPECT: method development and clinical validation in patients with no known coronary artery disease. Soc Nuclear Med; 2006. p. 51–8.
54. Slomka PJ, Nishina H, Abidov A, Hayes SW, Friedman JD, Berman DS, et al. Combined quantitative supine-prone myocardial perfusion SPECT improves detection of coronary artery disease and normalcy rates in women. J Nucl Cardiol. 2007;14(1):44–52. doi:10.1016/j.nuclcard.2006.10.021.
55. Nakajima K. Normal values for nuclear cardiology: Japanese databases for myocardial perfusion, fatty acid and sympathetic imaging and left ventricular function. Ann Nucl Med. 2010;24(3):125–35. doi:10.1007/s12149-009-0337-2.
56. Nakajima K, Matsuo S, Kawano M, Matsumoto N, Hashimoto J, Yoshinaga K, et al. The validity of multi-center common normal database for identifying myocardial ischemia: Japanese Society of Nuclear Medicine working group database. Ann Nucl Med. 2010;24(2):99–105. doi:10.1007/s12149-009-0331-8.
57. Nakajima K, Okuda K, Kawano M, Matsuo S, Slomka P, Germano G, et al. The importance of population-specific normal database for quantification of myocardial ischemia: comparison between Japanese 360 and 180-degree databases and a US database. J Nucl Cardiol. 2009;16(3):422–30. doi:10.1007/s12350-009-9049-1.
58.• Nakajima K, Matsumoto N, Kasai T, Matsuo S, Kiso K, Okuda K. Normal values and standardization of parameters in nuclear cardiology: Japanese Society of Nuclear Medicine working group database. Ann Nucl Med. 2016;30(3):188–99. doi:10.1007/s12149-016-1065-z. **This study conducted by the Japanese Society of Nuclear Medicine aims at building a population specific database for the japanese population. This population exhibits regional particularities that have to be taken into account for the normal databases generation**.
59. Li D, Li D, Feng J, Yuan D, Cao K, Chen J. Quantification of myocardial perfusion SPECT studies in Chinese population with Western normal databases. J Nucl Cardiol. 2010;17(3):486–93. doi:10.1007/s12350-010-9217-3.
60. Cuberas-Borros G, Aguade-Bruix S, Boronat-de Ferrater M, Muxi-Pradas MA, Romero-Farina G, Castell-Conesa J, et al. Normal myocardial perfusion SPECT database for the Spanish population. Rev Esp Cardiol. 2010;63(8):934–42.
61.•• Sonia Merlano-Gaitan FE. Russell Folks and Ernest Garcia. Diagnostic performance of a normal myocardial perfusion SPECT database specific for patients with end stage renal disease. the journal of nuclear medicine. 2014;55(1):1753. **This is the first disease-**

specific normal database reported. An effective normal database has been developed for patients with end-stage renal disease who have a myocardial perfusion disease-specific signature.

62. Jensen MD, Ryan DH, Apovian CM, Ard JD, Comuzzie AG, Donato KA, et al. 2013 AHA/ACC/TOS guideline for the management of overweight and obesity in adults: a report of the American College of Cardiology/American Heart Association Task Force on Practice Guidelines and The Obesity Society. J Am Coll Cardiol. 2014;63(25 Pt B):2985–3023. doi:10.1016/j.jacc.2013.11.004.
63. DePuey EG, Garcia EV. Optimal specificity of thallium-201 SPECT through recognition of imaging artifacts [see comments]. J Nucl Med. 1989;30(4):441–9.
64. DePuey 3rd EG. How to detect and avoid myocardial perfusion SPECT artifacts. J Nucl Med. 1994;35(4):699–702.
65. Gimelli A, Bottai M, Giorgetti A, Genovesi D, Filidei E, Marzullo P. Evaluation of ischaemia in obese patients: feasibility and accuracy of a low-dose protocol with a cadmium-zinc telluride camera. Eur J Nucl Med Mol Imaging. 2012;39(8):1254–61. doi:10.1007/s00259-012-2161-5.
66. Fiechter M, Gebhard C, Fuchs TA, Ghadri JR, Stehli J, Kazakauskaite E, et al. Cadmium-zinc-telluride myocardial perfusion imaging in obese patients. J Nucl Med. 2012;53(9):1401–6. doi:10.2967/jnumed.111.102434.

Terms and Conditions

Springer Nature journal content, brought to you courtesy of Springer Nature Customer Service Center GmbH (“Springer Nature”).
Springer Nature supports a reasonable amount of sharing of research papers by authors, subscribers and authorised users (“Users”), for small-scale personal, non-commercial use provided that all copyright, trade and service marks and other proprietary notices are maintained. By accessing, sharing, receiving or otherwise using the Springer Nature journal content you agree to these terms of use (“Terms”). For these purposes, Springer Nature considers academic use (by researchers and students) to be non-commercial.
These Terms are supplementary and will apply in addition to any applicable website terms and conditions, a relevant site licence or a personal subscription. These Terms will prevail over any conflict or ambiguity with regards to the relevant terms, a site licence or a personal subscription (to the extent of the conflict or ambiguity only). For Creative Commons-licensed articles, the terms of the Creative Commons license used will apply.
We collect and use personal data to provide access to the Springer Nature journal content. We may also use these personal data internally within ResearchGate and Springer Nature and as agreed share it, in an anonymised way, for purposes of tracking, analysis and reporting. We will not otherwise disclose your personal data outside the ResearchGate or the Springer Nature group of companies unless we have your permission as detailed in the Privacy Policy.
While Users may use the Springer Nature journal content for small scale, personal non-commercial use, it is important to note that Users may not:

1. use such content for the purpose of providing other users with access on a regular or large scale basis or as a means to circumvent access control;
2. use such content where to do so would be considered a criminal or statutory offence in any jurisdiction, or gives rise to civil liability, or is otherwise unlawful;
3. falsely or misleadingly imply or suggest endorsement, approval , sponsorship, or association unless explicitly agreed to by Springer Nature in writing;
4. use bots or other automated methods to access the content or redirect messages
5. override any security feature or exclusionary protocol; or
6. share the content in order to create substitute for Springer Nature products or services or a systematic database of Springer Nature journal content.

In line with the restriction against commercial use, Springer Nature does not permit the creation of a product or service that creates revenue, royalties, rent or income from our content or its inclusion as part of a paid for service or for other commercial gain. Springer Nature journal content cannot be used for inter-library loans and librarians may not upload Springer Nature journal content on a large scale into their, or any other, institutional repository.
These terms of use are reviewed regularly and may be amended at any time. Springer Nature is not obligated to publish any information or content on this website and may remove it or features or functionality at our sole discretion, at any time with or without notice. Springer Nature may revoke this licence to you at any time and remove access to any copies of the Springer Nature journal content which have been saved.
To the fullest extent permitted by law, Springer Nature makes no warranties, representations or guarantees to Users, either express or implied with respect to the Springer nature journal content and all parties disclaim and waive any implied warranties or warranties imposed by law, including merchantability or fitness for any particular purpose.
Please note that these rights do not automatically extend to content, data or other material published by Springer Nature that may be licensed from third parties.
If you would like to use or distribute our Springer Nature journal content to a wider audience or on a regular basis or in any other manner not expressly permitted by these Terms, please contact Springer Nature at

onlineservice@springernature.com